Islanding Detection of Synchronous Machine-Based DGs using Average Frequency Based Index

M. Bakhshi*, R. Noroozian* and G. B. Gharehpetian**

Abstract: Identification of intentional and unintentional islanding situations of Dispersed Generators (DGs) is one of the most important protection concerns in power systems. Considering safety and reliability problems of distribution networks, an exact diagnosis index is required to discriminate the loss of the main network from the existing parallel operation. Hence, this paper introduces a new islanding detection method for synchronous machine–based DGs. This method uses the average value of the generator frequency to calculate a new detection index. The proposed method is an effective supplement of the Over/Under Frequency Protection (OFP/UFP) system. The analytical equations and simulation results are used to assess the performance of the proposed method under various scenarios such as different types of faults, load changes and capacitor bank switching. To show the effectiveness of the proposed method, it is compared with the performance of both ROCOF and ROCOFOP methods.

Keywords: Islanding detection, Non-detection zone, Passive methods, Synchronous machine-based Distributed Generation (DG).

1 Introduction

Nowadays, DG has been broadly used in distribution power systems. It can supply electricity secure to customers, be active in a deregulation of the electricity market, increase the reliability and decrease environmental concerns [1, 2]. The islanding identification for the connection of distributed generators to distribution networks is an important issue. According to IEEE standard 1547-2003, the islanding condition is defined as a situation in which a part of an electric power system is solely energized and separated from the rest of the system [3]. Failure to islanding detection can lead to several negative impacts to the generators and connected loads, as follows [4, 5]:

1. The islanded grid cannot control its frequency and voltage. This earns result in equipment damages.
2. This condition may cause safety hazards to utility workers and customers.

Therefore, the islanding situation must be detected as soon as possible. Many islanding detection methods have been proposed, which can be classified into two main categories. Remote methods, such as power line communication [6] and supervisory control and data acquisition [7] methods. They do not have Non-Detection Zone (NDZ) and are more reliable than the local methods but more expensive. NDZs are defined as a loading condition for which an islanding detection method would fail to operate in a timely manner [8].

The local methods can be classified into two major groups: active and passive methods. According to the active methods, islanding is detected based on adding a perturbation signal into the system. The perturbation signals in parallel operation have no significant effect; but in the case of the loss of main grid, these signals are detected. Some of active methods, which have been recently introduced, include positive feedback for active and reactive power loops in governor and excitation system of synchronous DGs [9], injection a negative sequence of current through the interface Voltage-Sourced Converter (VSC) [10], Sandia frequency and voltage shift methods [11] and harmonic amplification factor, which is based on the voltage change at the Point of Common Coupling (PCC) [4].

Passive methods are based on measuring local parameters of DG and comparing it with preset value. Passive methods, which have been proposed, include Over/Under Frequency/Voltage Protections (OFP/UFP and OVP/UVP) and rate of change of frequency over the time [12-14]. Vector surge relay is the other

Iranian Journal of Electrical & Electronic Engineering, 2013.
Paper first received 24 Jan. 2013 and in revised form 10 Mar. 2013.
* The Authors are with the Department of Electrical Engineering, University of Zanjan, Zanjan.
** The Author is with the Electrical Engineering Department, Amirkabir University of Technology, Tehran, Iran.
E-maisl: bakhshi.mohsen@gmail.com, noroozian@znu.ac.ir and grptian@aut.ac.ir.

solution, which has been explained in [15]. Some of passive methods use two parameters simultaneously, e.g., rate of change of frequency over the active power [16] and rate of change of phase angle difference [17]. For inverter-based DGs, two new islanding detection methods based on using DC voltage and reference power of the DG has been considered in [8] and [18], respectively. Artificial Neural Network (ANN), Kalman Filtering (KF), estimation based methods, application of adaptive fuzzy and duffing oscillators are the other major methods, which are very efficient to detect the islanding situation. These methods, in both inverter-based and synchronous–machine based DGs, have been investigated in [19-24]. Although these methods are very effective but also have a lot of complexity. Classification-based islanding detection schemes, which have been recently developed, are passive methods reviewed in [25, 26]. The combination of different types of islanding detection techniques which are known as hybrid methods have been introduced in [5, 27, 28]. In [5, 27], the combination of both active and passive methods have been investigated whereas [28] expresses the combination of both communication and passive methods. Although the active methods have smaller NDZ than the passive methods but degrade the power quality of the system [18].

Most of the passive methods, monitoring only one parameter, have a large NDZ, while simultaneous monitoring of two parameters further decreases the NDZ of passive methods and have a small NDZ [16, 17]. In this paper, the average value of the frequency is used to reduce NDZ of OFP/UFP. The proposed method uses only one parameter to detect islanding situation and from the viewpoint of reducing the NDZ, it has the same performance and capability as two parameters monitoring methods.

The paper is organized as follows: the proposed method is described in section 2. Section 3 shows the results of simulations and discussions. In section 4 comparison of proposed method with two passive methods is carried out and finally section 5 represents the conclusions.

2 Proposed Method

2.1 Frequency Deviation for Grid-Connected and Islanded Modes

For a Synchronous Distributed Generator (SDG), which is operating in parallel with a utility main network and feeds the local load, the following swing equation is defined [30, 31]:

$$\frac{2H}{\omega_b}\frac{d\omega}{dt} = P_m - P_e - D\omega \tag{1}$$

where, H, ω_b, D, P_m and P_e are generator inertia constant, synchronous speed of DG, damping coefficient, mechanical and electrical power of the DG, respectively. The swing equation must be solved for two different modes; parallel operation with main network and loss of main network.

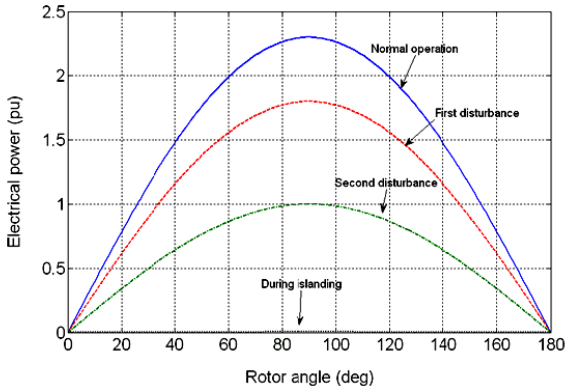

Fig. 1 Synchronizing coefficient in different conditions.

1) Grid-Connected Mode of SDG

In this mode, based on the manipulation of Eq. (1), presented in appendix, the following equation can be written:

$$\frac{2H}{\omega_b}\frac{d^2\Delta\delta}{dt^2} + D\frac{d\Delta\delta}{dt} = -P_{\max}\cos(\Delta\delta) \tag{2}$$

where, the term $P_{\max}\cos(\Delta\delta)$ is known as synchronizing coefficient. This parameter has a very important role in the dynamic behavior of the synchronous generator. Fig. 1, shows the values of the synchronizing coefficient in different conditions of the power system. By solving Eq. (2) and considering $\Delta\delta(0) = \Delta\delta_0$ and $\Delta\omega(0) = 0$ as initial conditions, following responses for frequency and rotor angle deviations can be obtained:

$$\Delta\delta(t) = \frac{\Delta\delta_0}{\sqrt{1-\varsigma^2}} e^{-\varsigma\omega_n t}\sin(\omega_d t + \theta) \tag{3}$$

$$\Delta f(t) = \frac{-\omega_n \Delta\delta_0}{2\pi\sqrt{1-\varsigma^2}} e^{-\varsigma\omega_n t}\sin(\omega_d t) \tag{4}$$

where, we have:

$$\omega_n = \sqrt{\frac{P_{\max}\cos(\delta_0).\omega_b}{2H}} \tag{5}$$

$$\varsigma = \frac{D}{2}\sqrt{\frac{\omega_b}{2H.P_{\max}\cos(\delta_0)}} \tag{6}$$

$$\omega_d = \omega_n\sqrt{1-\varsigma^2} \tag{7}$$

$$\theta = \cos^{-1}(\varsigma) \tag{8}$$

Considering Eq. (3) and Eq. (4), it can be said that the frequency and rotor angle deviations have a damped sinusoidal waveform and after a while the amplitude of these signals will be equal to the zero.

2) Loss of Main Grid:

In this mode, the response of the frequency to a loss of main grid is determined. In the islanding situation, the transmitted power between DG and main network reaches to zero (see Fig. 1). It means that the synchronizing coefficient $P_{\max}\cos(\Delta\delta)$ must be equal to zero. Therefore, in Eq. (2), we have:

$$\frac{2H}{\omega_b}\frac{d^2\Delta\delta}{dt^2}+D\frac{d\Delta\delta}{dt}=0 \tag{9}$$

By solving Eq. (9) with $\Delta\delta(0)=\Delta P\omega_b/2H$ and $\Delta\omega(0)=2\pi\Delta P/D$ as initial conditions, the following response for frequency deviations can be obtained:

$$\Delta f(t)=\frac{\Delta P}{D}\left(1-e^{-2\zeta\omega_n t}\right) \tag{10}$$

Here, ΔP is the active power imbalance. By comparing Eq. (4) and Eq. (10), it can be seen that frequency deviations in grid-connected and islanded modes are different. When the real power mismatches (ΔP) causes transients in the islanded portion, the frequency of DG increases or decreases. Therefore, the aforementioned frequency deviations can be used to detect the islanding condition.

2.2 Fundamentals of Proposed Method

In this section, the average value of the frequency (i.e., Δf_{mean}) is determined and a new detection index is introduced. The average value of the frequency deviation is written, as follows:

$$\Delta f_{mean}=\frac{1}{T_d}\int_0^{T_d}\Delta f(t).dt \tag{11}$$

where, T_d is the fundamental period of the frequency deviation determined by Eq. (7), as follows:

$$\omega_d=2\pi f_d=\frac{2\pi}{T_d}\Rightarrow T_d=\frac{2\pi}{\omega_n\sqrt{1-\zeta^2}} \tag{12}$$

Now, Eq. (11) should be calculated for both operation modes.

a) For grid-connected mode, by Eq. (4) and Eq. (11), the frequency deviation will be determined, as follows:

$$\Delta f_{mean-on}=\frac{1}{T_d}\int_0^{T_d}-\frac{\omega_n\Delta\delta_0}{2\pi\sqrt{1-\zeta^2}}e^{-\zeta\omega_n t}\sin(\omega_d t).dt$$

$$=\frac{1}{T_d}\frac{-\omega_n\Delta\delta_0}{2\pi\sqrt{1-\zeta^2}}\left[\frac{\omega_d\left(1-e^{-\zeta\omega_n T_d}\right)}{(\zeta\omega_n)^2+\omega_d^2}\right] \tag{13}$$

Using Eq. (7), the simpler form can be obtained, as follows:

$$\Delta f_{mean-on}=\frac{-\Delta\delta_0}{2\pi T_d}\left[1-e^{-\zeta\omega_n T_d}\right] \tag{14}$$

where, $\Delta\delta_0$ is the initial rotor angle deviation which can be created in different disturbances of the power systems.

b) For islanding condition, by Eq. (10) and Eq. (11), the frequency deviation will be calculated, as follows:

$$\Delta f_{mean-off}=\frac{1}{T_d}\int_0^{T_d}\frac{\Delta P}{D}\left(1-e^{-2\zeta\omega_n t}\right)dt$$

$$=\frac{\Delta P}{T_d.D}\left[T_d+\frac{1}{2\zeta\omega_n}e^{-2\zeta\omega_n T_d}-\frac{1}{2\zeta\omega_n}\right] \tag{15}$$

To analyze the performance of the proposed method and assessment of its Non–Detection Zone (NDZ), the critical power imbalance of the method must be calculated. The critical power imbalance is the minimum power deviation which one islanding detection method can discriminate between two operation modes using it. The mentioned power deviation is described as a difference between produced and absorbed electrical power by DGs and loads, respectively.

The critical power imbalance of the proposed method is determined by the following inequality:

$$\left|\frac{\Delta f_{mean-off}}{\Delta f_{mean-on}}\right|>1 \tag{16}$$

Eq. (16), can be rewritten, as follows:

$$\left|\frac{\frac{\Delta P}{T_d.D}\left[T_d+\frac{1}{2\zeta\omega_n}e^{-2\zeta\omega_n T_d}-\frac{1}{2\zeta\omega_n}\right]}{\frac{-\Delta\delta_0}{2\pi T_d}\left[1-e^{-\zeta\omega_n T_d}\right]}\right|>1 \tag{17}$$

This inequality can be also written in the following form:

$$\Delta P>\left|\frac{\Delta\delta_0 D}{2\pi}\frac{\left[1-e^{-\zeta\omega_n T_d}\right]}{\left[T_d+\frac{1}{2\zeta\omega_n}e^{-2\zeta\omega_n T_d}-\frac{1}{2\zeta\omega_n}\right]}\right|=|\psi| \tag{18}$$

Then, the non-detection zone of proposed method is introduced, as follows:

$$-\psi<\Delta P_{NDZ}<\psi \tag{19}$$

To study the performance of the proposed method, the critical power imbalance (i.e., $\Delta P_{critical}=\psi$) and the coefficient $k=\zeta\omega_n T_d$ should be considered. The time

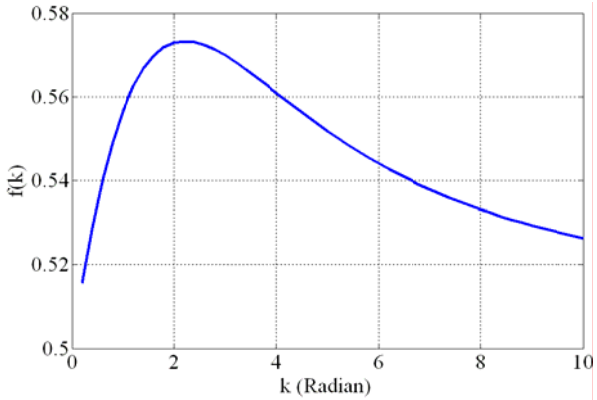

Fig. 2 Variation of $f(k)$ versus k.

constant of the frequency deviation signal is represented by $\tau = 1/\zeta\omega_n$ and for all damped sinusoidal signals, the settling time is about four times of the time constant (i.e., $t_{settling} = 4/\zeta\omega_n$) [32]. In the other words, the settling time of the frequency deviation signal is about 2 to 8 times of the fundamental period. Therefore, we have:

$$0.5 < \varsigma\omega_n T_d < 2 \quad or \quad 0.5 < k < 2 \tag{20}$$

Using Eq. (18), the critical active power imbalance can be expressed by the following equation:

$$\psi = \frac{\Delta\delta_0 D}{\pi T_d} f(k) \tag{21}$$

where, $f(k)$ is defined, as follows:

$$f(k) = \frac{k\left(1 - e^{-k}\right)}{(2k-1) + e^{-2k}} \tag{22}$$

Fig. 2, shows $f(k)$ versus k. According to this figure, the maximum value of $f(k)$ is 0.5733 at $k = 2.2$. So, the worst case is $f(2) = 0.5729$ for ψ. In Eq. (21), $\Delta\delta_0$ is the initial rotor angle deviation that occurs in the presence of a disturbance in the power network. This parameter is in radian and it can be converted into degree. Then, Eq. (21) can be rewritten, as follows:

$$\psi = \frac{\Delta\delta_0}{180}\frac{D}{T_d} \times 0.5729 \tag{23}$$

In Eq. (23), D/T_d is an important parameter which has a vital role to reduce NDZ of the proposed method. Although, D/T_d is characterized by all of parameters of the synchronous distributed generator and has different values but its range can be estimated. To achieve a NDZ smaller than 5 percent in the proposed method for different types of synchronous distributed generators, D/T_d is better to be lower than 1. In the following paragraphs, it will be shown that D/T_d in existing synchronous distributed generators is smaller than 1. From Eq. (5) and Eq. (6) the following equations can be written:

$$\varsigma\omega_n = \frac{D\omega_b}{4H} \Rightarrow D = \frac{4H.\varsigma\omega_n}{\omega_b}$$

$$or, \quad T_d D = \frac{4H(T_d\varsigma\omega_n)}{\omega_b} = \frac{4H}{\omega_b}k$$

$$or, \quad \frac{D}{T_d} = \frac{4k}{\omega_b}\left(\frac{H}{T_d^2}\right) \tag{24}$$

where, ω_b and H are synchronous speed of DG and inertia constant, respectively. For $k = 2$ and $\omega_b = 2\pi.60$, the worst case for the biggest value of D/T_d is, as follows:

$$\frac{D}{T_d} \cong 0.0212\left(\frac{H}{T_d^2}\right) \tag{25}$$

In this equation, H is an important parameter to evaluate the D/T_d. According to [30, 31], $0.5^s \le H \le 10^s$. This constant depends on the machine size. Hence, H of synchronous distributed generators in distribution networks is lower than four [9, 13, 25, 29]. Then, the fundamental period of the frequency deviation or T_d, is changed from 0.15 to 1.5s. For example, in the case study, which will be presented in the next section, H = 1.5s and T_d = 0.33s. Thus, we have:

$$\frac{D}{T_d} \cong 0.0212\left(\frac{1.5}{0.33^2}\right) \cong 0.292 \tag{26}$$

As it can be seen the result is smaller than one. It should be noted that T_d is proportional to H. this means that the high value of H needs more time for oscillations. In Fig. 3, the rotor speed variations for four different values of inertia constant of one typical synchronous DG have been simulated and shown. D/T_d for four cases has been determined, as follows:

$$For \begin{cases} H = 0.5 \\ T_d = 0.22 \end{cases} \Rightarrow \frac{D}{T_d} \cong 0.2190 \tag{27}$$

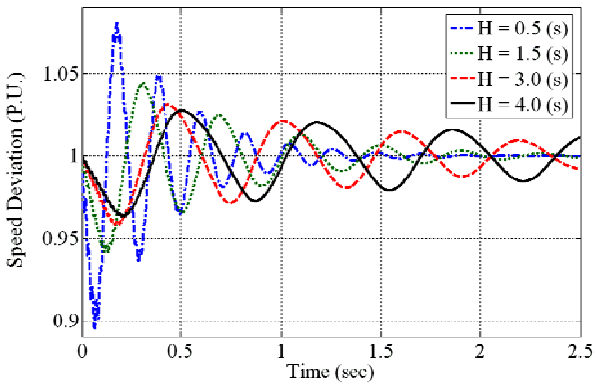

Fig. 3 Behavior of rotor speed deviation for different H.

$$For \quad \begin{cases} H = 1.5 \\ T_d = 0.4 \end{cases} \Rightarrow \frac{D}{T_d} \cong 0.19875 \tag{28}$$

$$For \quad \begin{cases} H = 3.0 \\ T_d = 0.6 \end{cases} \Rightarrow \frac{D}{T_d} \cong 0.17\overline{6} \tag{29}$$

$$For \quad \begin{cases} H = 4.0 \\ T_d = 0.7 \end{cases} \Rightarrow \frac{D}{T_d} \cong 0.17306 \tag{30}$$

Considering the aforementioned results, it can be said that D/T_d for the most of DGs is smaller than one and in the worst case, it is equal to 1. Consequently, $D/T_d = 1$ can be substituted in Eq. (23), as follows:

$$\psi = 0.5729 \frac{\Delta\delta_0}{180} \tag{31}$$

In this equation, $\Delta\delta_0$ has a vital role to determine the limits of islanding and non–islanding conditions. To illustrate the discrimination procedure of the proposed method, the following two criterions must be considered.

1. If $\Delta\delta_0 \leq 10°$

For this condition, the frequency variations certainly are in acceptable range (i.e., $59.3^{Hz} \leq f \leq 60.5^{Hz}$) [3]. Thus, over/under frequency protections will not operate. Consequently, NDZ could be written, as follows:

$$\psi(pu) \leq 0.5729 \frac{10}{180} \cong 0.03182$$

$$\psi \leq 3.182\% \tag{32}$$

2. If $\Delta\delta_0 \geq 10°$

For this situation, frequency probably exceeds its acceptable range and over/under frequency protections for more cases will operate. If frequency variations were remained in acceptable range, NDZ of the method could be achieved, as follows:

$$\psi(pu) \geq 0.5729 \frac{10}{180} \cong 0.03182$$

$$\psi \geq 3.182\% \tag{33}$$

2.3 Procedure of Proposed Method

In this subsection, the calculation procedure of f_{mean} is described. To calculate the f_{mean}, both procedures, i.e. the voltage zero crossing and the rotor speed have used. After the computation of f_{mean}, the detection index is calculated, as follows:

$$D_{on/off} = k_g \cdot \left| \Delta f_{mean-on/off} \right| \tag{34}$$

where, Δf_{mean} is ($f_b - f_{mean}$) and f_b and D are the fundamental frequency and the detection index of the proposed method, respectively. The k_g is a gain, adjusted to 100. The flowchart of the proposed method is shown in Fig. 4. In this figure, D_{th1} is the first threshold value of the detection index, which can be acquired from comparing islanding and non- islanding cases. Using Eqs. (14) and (15) for $\Delta P = 3\%$ and $\Delta\delta_0 = 10^{\circ}$, different detection parameters have been represented in Table 1.

Table 1. Detection indices for both case study systems.

		D_{on}*	D_{off}	D_{th1}	D_{th2}
First system	**SDG**	8.10	10.32	8	32
Second system	**Gas Turbine**	9.62	12.86	9	36
	Diesel Generator	10.37	13.42	10	40

*The unit of D is Hertz.

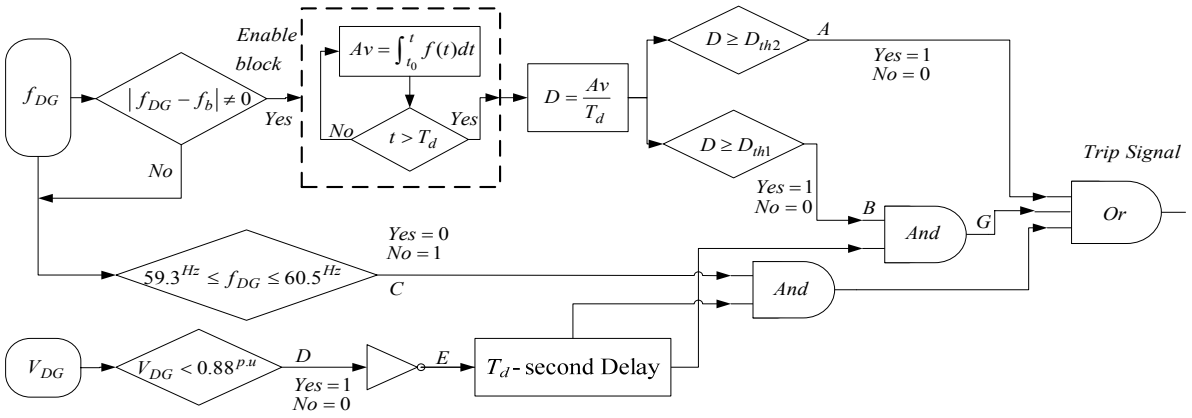

Fig. 4 Flowchart of proposed method.

3 Simulation Results and Discussion

To verify the effectiveness of the proposed method, various islanding and non-islanding occurrences have been applied on the case study systems as shown in Figs. 5 and 6. For both under study systems, sixth–order model of SDG for simulations is used. More information about first and second case study systems can be found in [12] and [29], respectively. It should be noted that all simulations have been carried out in Matlab/SimPowerSystem software environment. The most important disturbances which may result in wrong performance of islanding detection methods are short circuit faults, load variations and capacitor bank switching. In this paper, 55 different islanding and non–islanding cases have been studied by the proposed

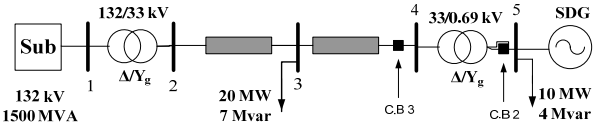

Fig. 5 Single line diagram of first case study system.

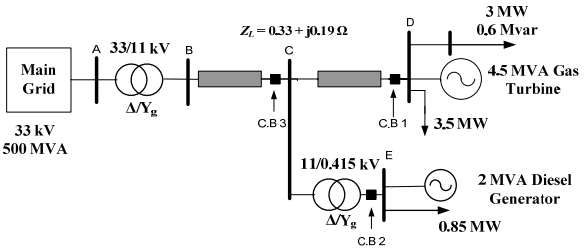

Fig. 6 Single line diagram of second case study system.

Table 2. Classification of different islanding and non-islanding conditions using proposed method on the first system.

Disturbance	Explain	f_{mean} (Hz)	D (Hz)	Exceeds from V_{min}	Detection by	Classification
Three phase to ground faults (ohm)	$R_f = 11$ $R_f = 15$ $R_f = 20$ $R_f = 1$	59.81194 59.83105 59.86752 59.76596	18.806 16.895 13.248 23.404	Yes Yes Yes Yes	UVP UVP UVP UVP	Non- islanding
Double line to ground faults (ohm)	$R_f = 7$ $R_f = 15$ $R_f = 30$	59.81310 59.91235 59.95681	18.690 8.765 4.319	Yes Yes Yes	UVP UVP UVP	Non- islanding
Single line to ground faults (ohm)	$R_f = 5$ $R_f = 10$ $R_f = 20$	59.88311 59.91728 59.94312	11.689 8.272 5.688	Yes Yes No	UVP UVP D_{th1}	Non- islanding
Capacitor switching off (Mvar)	$Q_C = 40$ $Q_C = 30$ $Q_C = 20$	59.99552 60.00198 60.00030	0.448 0.198 0.030	No No No	D_{th1} D_{th1} D_{th1}	Non- islanding
Capacitor switching on (Mvar)	$Q_C = 40$ $Q_C = 30$ $Q_C = 20$	60.00876 60.00793 60.00521	0.876 0.793 0.521	No No No	D_{th1} D_{th1} D_{th1}	Non- islanding
RLC load switching off (MW + j Mvar)	$S = 40 + j\ 30$ $S = 30 + j\ 20$ $S = 20 + j\ 10$	59.98999 60.00992 60.00705	1.001 0.992 0.705	No No No	D_{th1} D_{th1} D_{th1}	Non- islanding
RLC load switching on (MW + j Mvar)	$S = 40 + j\ 30$ $S = 30 + j\ 20$ $S = 20 + j\ 10$	60.01895 59.99190 59.99333	1.895 0.810 0.667	No No No	D_{th1} D_{th1} D_{th1}	Non- islanding
C.B2 or C.B3 switching off (percent)	$\Delta P = 2.7$ $\Delta Q = 4$	60.18375	18.375	No	D_{th1}	Islanding
C.B2 or C.B3 switching off (percent)	$\Delta P = -2$ $\Delta Q = 8$	59.84654	15.346	No	D_{th1}	Islanding
C.B2 or C.B3 switching off (percent)	$\Delta P = 8$ $\Delta Q = -3$	60.60548	60.548	No	D_{th1} & D_{th2}	Islanding
C.B2 or C.B3 switching off (percent)	$\Delta P = 40$ $\Delta Q = 60$	63.82078	382.078	Yes	OFP& D_{th2}	Islanding
C.B2 or C.B3 switching off (percent)	$\Delta P = 3.3$ $\Delta Q = 0$	60.21956	21.956	No	D_{th1}	Islanding
C.B2 or C.B3 switching off (percent)	$\Delta P = -6$ $\Delta Q = -5.5$	59.58752	41.248	No	D_{th1}	Islanding
C.B2 or C.B3 switching off (percent)	$\Delta P = -16.5$ $\Delta Q = 10$	59.05327	94.673	No	D_{th1} & D_{th2}	Islanding

Table 3. Classification of different *Islanding* conditions using proposed method on the second system.

Disturbance	Explain	D_{DG1}(Hz)	D_{DG2}(Hz)	Exceeds from $V_{min}1$	Exceeds from $V_{min}2$	Detection by	Classification
C.B1 switching off (percent)	$\Delta P_1 = 3$ $\Delta Q_1 = -5$	16.650	0.0635	No	No	D_{th1}	Islanding of DG_1
C.B1 switching off (percent)	$\Delta P_1 = 2.5$ $\Delta Q_1 = 3$	10.320	0.0638	No	No	D_{th1}	Islanding of DG_1
C.B1 switching off (percent)	$\Delta P_1 = -60$ $\Delta Q_1 = 25$	303.20	0.0843	No	No	*UFP* & D_{th1}	Islanding of DG_1
C.B1 switching off (percent)	$\Delta P_1 = 25$ $\Delta Q_1 = -25$	37.527	0.1270	Yes	Yes	D_{th2}	Islanding of DG_1
C.B1 switching off (percent)	$\Delta P_1 = 40$ $\Delta Q_1 = 5$	177.81	0.3611	Yes	Yes	*OFP* & D_{th2}	Islanding of DG_1
C.B2 switching off (percent)	$\Delta P_2 = 4.5$ $\Delta Q_2 = -4$	31.280	0.0921	No	No	D_{th1}	Islanding of DG_2
C.B2 switching off (percent)	$\Delta P_2 = -3$ $\Delta Q_2 = -1$	13.120	0.0484	No	No	D_{th1}	Islanding of DG_2
C.B2 switching off (percent)	$\Delta P_2 = 3.2$ $\Delta Q_2 = 3$	22.850	0.0658	No	No	D_{th1}	Islanding of DG_2
C.B2 switching off (percent)	$\Delta P_2 = 2$ $\Delta Q_2 = 3$	13.390	0.0339	No	No	D_{th1}	Islanding of DG_2
C.B2 switching off (percent)	$\Delta P_2 = -16$ $\Delta Q_2 = 5$	89.490	0.2626	No	No	*UFP* & D_{th1}	Islanding of DG_2
C.B2 switching off (percent)	$\Delta P_2 = 55$ $\Delta Q_2 = -33$	306.50	1.5450	yes	yes	D_{th2}	Islanding of DG_2
C.B3 switching off (percent)	$\Delta P_1 = 8$ $\Delta Q_1 = -10$ $\Delta P_2 = 10$ $\Delta Q_2 = -8$	53.140	54.610	No	No	D_{th1}	Islanding of both DG_1 and DG_2
C.B3 switching off (percent)	$\Delta P_1 = 5$ $\Delta Q_1 = -8$ $\Delta P_2 = 7$ $\Delta Q_2 = -6$	32.091	33.045	No	No	D_{th1}	Islanding of both DG_1 and DG_2
C.B3 switching off (percent)	$\Delta P_1 = -2.5$ $\Delta Q_1 = 2$ $\Delta P_2 = -2.5$ $\Delta Q_2 = 2$	11.950	12.389	No	No	D_{th1}	Islanding of both DG_1 and DG_2

method. The phase–locked loop block with three phase voltage of DG is used to achieve the frequency waveform. From Fig. 4, the proposed method has been introduced as supplementary protection of Over/Under Frequency Protection (OFP/UFP). To prevent sending of any undesired trip signal for sever disturbances like three phases faults, Under Voltage Protection (UVP) has also been used. The acceptable range of voltage is 0.88 pu–1.1 pu [3]. In the case of frequency and regarding the IEEE standard–1547, variations should be in the range of 59.3-60.5 Hz [3]. The simulated short circuit faults are Single Line to Ground (SLG), Double Line to Ground (DLG) and three phases with different fault resistances. It should be noted that the short circuit duration of all faults is 6 cycles and both islanding and non–islanding disturbances start at $t = 2$s.

Eventually, Tables 2-4, present the detection index for all of the disturbances. Table 2, depicts the tested results of the proposed method on the first case study system and Tables 3, 4 are related to the second case study system.

In these tables, the subscript "1" and "2" indicates gas turbine and diesel generator on the second case study systems. From Table 2, although, it can be seen for more faults, the detection index exceeds from first threshold but UVP detects these disturbances as non-

Table 4. Classification of different *Non–islanding* conditions using proposed method on the second system.

Disturbance	Explain	D_{DG1} (Hz)	D_{DG2} (Hz)	Exceeds from $V_{min}1$	Exceeds from $V_{min}2$	Detection by	Classification
Three phase to ground faults (ohm) line CD	$R_f = 5$	1.7040	8.9760	Yes	Yes	UVP	Non- islanding
	$R_f = 10$	2.0429	3.5384	Yes	Yes	UVP	
Three phase to ground faults (ohm) line BC	$R_f = 5$	1.2720	8.5436	Yes	Yes	UVP	Non- islanding
	$R_f = 10$	1.2174	3.6059	Yes	Yes	UVP	
Three phase to ground faults (ohm) bus D	$R_f = 5$	2.0634	8.8741	Yes	Yes	UVP	Non- islanding
	$R_f = 10$	2.9223	3.3374	Yes	Yes	UVP	
DLG faults (ohm) line CD	$R_f = 5$	1.9375	4.7761	Yes	Yes	UVP	Non- islanding
	$R_f = 10$	1.3308	2.2294	Yes	Yes	UVP	
DLG faults (ohm) line BC	$R_f = 5$	1.1524	4.9517	Yes	Yes	UVP	Non- islanding
	$R_f = 10$	0.7544	2.3576	Yes	Yes	UVP	
DLG faults (ohm) bus D	$R_f = 5$	2.6814	4.4321	Yes	Yes	UVP	Non- islanding
	$R_f = 10$	2.0084	2.0213	Yes	Yes	UVP	
SLG faults (ohm) line CD	$R_f = 5$	1.1445	1.7914	Yes	Yes	UVP	Non- islanding
	$R_f = 10$	0.6507	1.0024	No	No	D_{th1}	
SLG faults (ohm) line BC	$R_f = 5$	0.6352	2.0487	Yes	Yes	UVP	Non- islanding
	$R_f = 10$	1.1770	0.3412	No	No	D_{th1}	
SLG faults (ohm) bus D	$R_f = 5$	1.6968	1.5290	Yes	Yes	UVP	Non- islanding
	$R_f = 10$	0.8753	0.9982	No	No	D_{th1}	
Capacitor switching off (Mvar) on bus C	$Q_C = 6$	0.1045	0.3061	No	No	D_{th1}	Non- islanding
	$Q_C = 4$	0.0523	0.1959	No	No	D_{th1}	
	$Q_C = 2$	0.0070	0.0823	No	No	D_{th1}	
Capacitor switching on (Mvar) on bus C	$Q_C = 6$	0.1390	0.2236	No	No	D_{th1}	Non- islanding
	$Q_C = 4$	0.1117	0.1548	No	No	D_{th1}	
	$Q_C = 2$	0.0869	0.0924	No	No	D_{th1}	
RLC load switching off (MW + j Mvar) on bus E	$S = 6 + j\,4$	0.0569	0.0212	No	No	D_{th1}	Non- islanding
	$S = 4 + j\,2$	0.0478	0.0184	No	No	D_{th1}	
	$S = 2 + j\,1$	0.0358	0.0152	No	No	D_{th1}	
RLC load switching on (MW + j Mvar) on bus E	$S = 6 + j\,4$	0.0575	0.0233	No	No	D_{th1}	Non- islanding
	$S = 4 + j\,2$	0.0483	0.0196	No	No	D_{th1}	
	$S = 2 + j\,1$	0.0371	0.0168	No	No	D_{th1}	
RLC load switching off (MW + j Mvar) on bus D	$S = 6 + j\,4$	0.1031	0.1224	No	No	D_{th1}	Non- islanding
	$S = 4 + j\,2$	0.1285	0.0549	No	No	D_{th1}	
	$S = 2 + j\,1$	0.0502	0.0474	No	No	D_{th1}	
RLC load switching on (MW + j Mvar) on bus D	$S = 6 + j\,4$	0.0476	0.1514	No	No	D_{th1}	Non- islanding
	$S = 4 + j\,2$	0.0360	0.1469	No	No	D_{th1}	
	$S = 2 + j\,1$	0.0248	0.1273	No	No	D_{th1}	

islanding conditions. In this paper, averaging time in all of the simulations has been adjusted to $t = T_d$ s. According to the IEEE standard–1547, the maximum allowable time to detect the islanding situation is 2s. Typically, the time of the islanding detection depends upon the magnitude of active and reactive power imbalances. For small power mismatches, the islanding situation should be detected within two seconds whereas for large power mismatches, this time is reduced to 0.160s. The amount of T_d is different for various types of synchronous machine–based DGs. For example, in first case study system, DG has a T_d of 0.338s and for second case study, T_{d1}=0.280s and T_{d2}=0.275s. For these cases (i.e., T_d > 160ms), it is better to use the OFP/UFP with the proposed method, because in large power mismatches, OFP/UFP has good performance and can detect the islanding condition quickly (i.e, $t < 160^{ms}$) [21]. These conditions have been shown in Table 2 and 3 for large values of ΔP and ΔQ. The coordination of the OFP/UFP and proposed method result in a better

performance and lesser NDZ. In the case of second system and at the first attempt, both SDGs have been islanded, separately. For this situation, the proposed method operated, excellently. For second attempt, both gas turbine and diesel generator have been islanded, simultaneously. In this condition the proposed method could detect the islanding events with active power imbalances up to 2.5%.

4 Comparison of Proposed Method with Two Passive Methods

4.1 ROCOF Method

The ROCOF relay is a simple method to detect the islanding conditions, which is considered by many utilities. Although, the implementation of this method is very simple and cheaper than the other methods but in small power mismatches has a poor performance and cannot correctly detect the islanding condition. Thus, in this paper, the proposed method is compared with ROCOF relay. According to this method, the rate of change of frequency after crossing of a 1st order filter is computed and it is compared with a preset threshold value. The 1st order filter is used to reduce high frequency transients. It should be noted that before sending a trip signal, the terminal voltage of DG must be compared with a V_{Min} to prevent an undesired trip, which is caused by generator startup and short circuit faults. The threshold value of the ROCOF relay is changed between 0.3 Hz/s to 2.5 Hz/s. Therefore, in this study by considering many scenarios such as short circuit faults, capacitor bank switching and load changing; threshold value is selected to 2 Hz/s. Figs. 7-10, depict the trip signals of proposed method and ROCOF relay for special islanding and non–islanding conditions. In this figures, it can be seen that for –2% and +3.3% of active power mismatches, the ROCOF relay has a poor performance and cannot detect the islanding conditions.

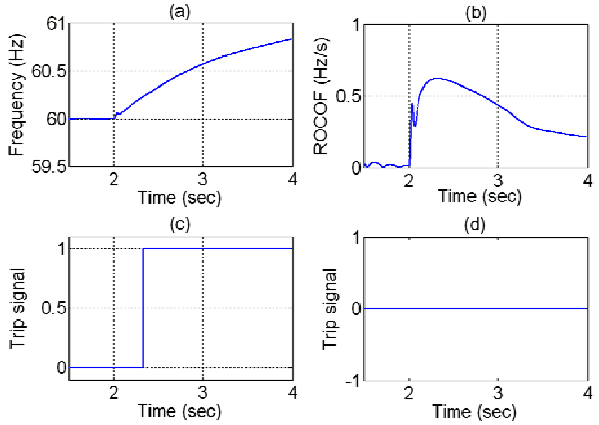

Fig. 7 Frequency of DG (a), output of ROCOF (b), trip signal of proposed method (c) and trip signal of ROCOF relay (d) in islanding conditions with ΔP=3.3% and ΔQ=0% at first system.

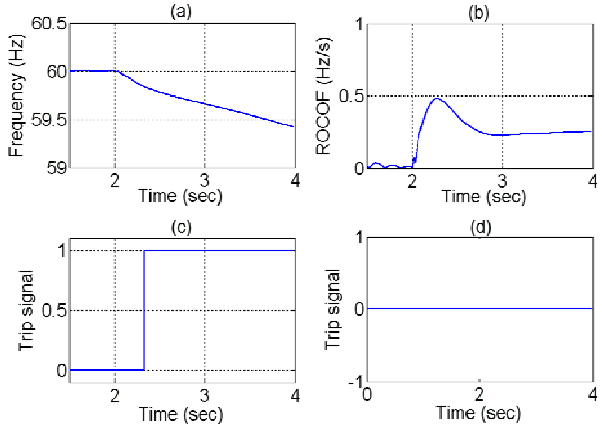

Fig. 8 Frequency of DG (a), output of ROCOF (b), trip signal of proposed method (c) and trip signal of ROCOF relay (d) in islanding conditions with ΔP=–2 % and ΔQ=8% at first system.

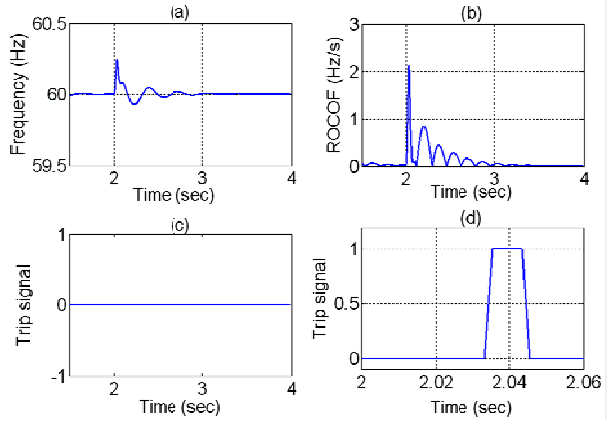

Fig. 9 Frequency of DG (a), output of ROCOF (b), trip signal of proposed method (c) and trip signal of ROCOF relay (d) for 30 MW and 20 Mvar of load shedding at first system.

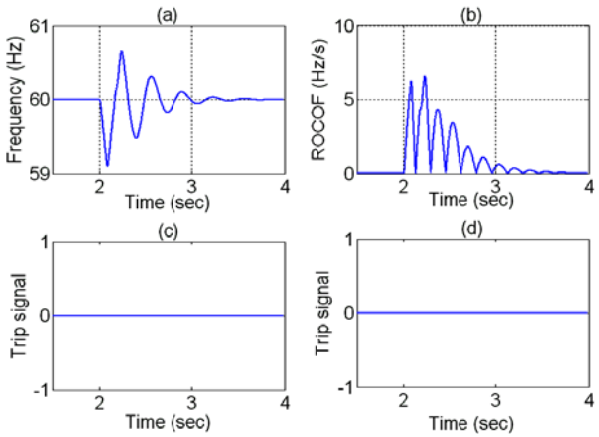

Fig 10. Frequency of DG (a), output of ROCOF (b), trip signal of proposed method (c) and trip signal of ROCOF relay (d) for three phases fault with R_f = 1 ohm at first system.

The NDZ of ROCOF relay in same conditions for both proposed method and ROCOF relay is more than 10%. Fig. 9 shows the wrong decision of ROCOF relay for a sample of load shedding. Finally, Fig. 10 depicts the correct decision of proposed method, when encountered with sever disturbance. As a result, although the ROCOF relay in large power mismatches (larger than 10% of active power mismatches) has a good performance and can quickly detect the islanding conditions but has a large NDZ.

4.2 Rate of Change of Frequency over Power

This method was introduced for the first time in [16]. Unlike of the ROCOF method, this procedure is more sensitive and has lower NDZ than the ROCOF. Also, this technique has two different threshold preset values. Thus, adjusting of these two parameters is rather difficult problem. Overall procedure of rate of change of frequency over power (ROCOFOP) method is based on comparing of output signal with first threshold; in this case, if output value of signal is larger than the first threshold, an embedded counter is incremented by one. Finally, by encroachment of counter value from second threshold, ROCOFOP proceeds to send a trip command. In the paper, this method is implemented in

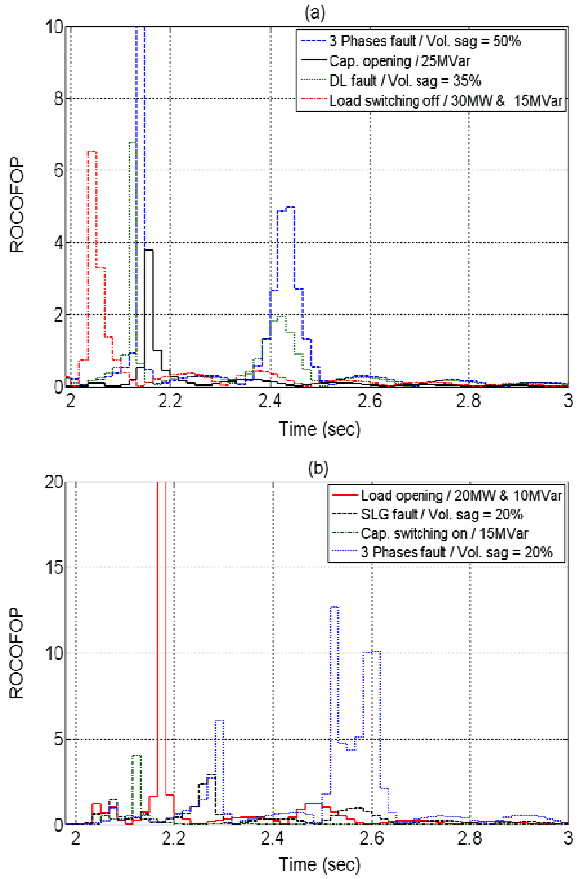

Fig. 11 Output results of ROCOFOP for non–islanding situations at first system.

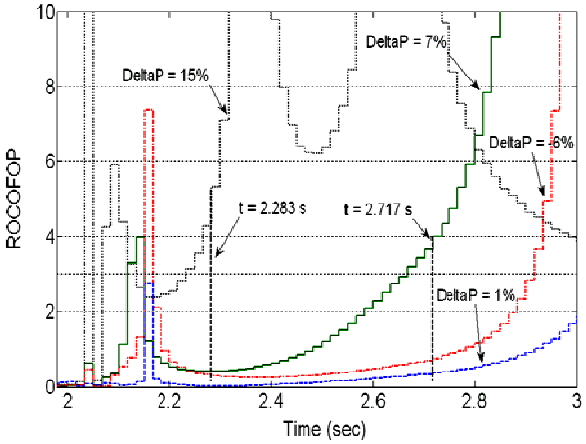

Fig 12. Output results of ROCOFOP for a few of islanding situations at first system.

Matlab environment on the case study system. The sample results of this method are depicted in Figs. 11 and 12. To reduce the false trip commands for non-islanding situations, the first and second thresholds are adjusted to 3 and 4, respectively. These threshold values are selected based on simulation results of different non-islanding situations. For the larger values than the adjusted values, in the case of thresholds, both parameters of detection time and NDZ criteria are increased. On the other hand, the lower values create false trips. Thus, in the paper, with these adjusted values for thresholds, the ROCOFOP method has an undesired trip for a special three phase fault. This status has been shown in Fig. 11-b. According to this figure, when the ROCOFOP method encounters with three phases fault, sends a trip command. This disturbance describes voltage sag, which causes a SDG terminal voltage drop of 20%. The time for all faults is six cycles. Fig. 12 depicts the results of the ROCOFOP method in islanding conditions. It is obvious that the ROCOFOP method has relatively large NDZ. For islanding condition with ΔP = 15%, this method can detect the islanding condition within 0.283s. For lower values, the performance of the ROCOFOP is reduced but in comparison with ROCOF, it is the better choice. For example, the ROCOFOP method can detect the islanding condition with ΔP = 7% within 0.717s, whereas the proposed method with ΔP = 2.7% and the detection time of 0.338s (first system) for islanding condition has robust performance. Also, for larger than 5% of active power mismatches, the ROCOFOP method can detect the islanding in more than 1s, whereas the proposed method for the same condition has the detection time of 0.338s (first system). It is necessary to note that for implementation of the ROCOFOP method, its output signal must be discrete. The discretisation process has been carried out through one Zero–Order–Hold (ZOH) filter. In this paper, this process with frequency of f_b, which is adjusted to 60 Hz, has been accomplished. Eventually, the proposed method in comparison with two typical passive methods is

effective and has a robust performance and good capability to detect the islanding conditions with small active power mismatches up to 3%.

5 Conclusion

This paper has proposed a new islanding detection method based on average value of frequency. By monitoring the frequency of the DG and calculating its average value, the proposed method can detect the islanding situation. Although this method is an integral–based method and has a rather long detection time but in comparison with derivative-based methods (e.g., ROCOF and ROCOFOP) has small NDZ. In fact, the proposed method is an effective supplement for OFP/UFP, which can reduce NDZ of OFP/UFP to less than 3%. To evaluate the performance and capability of the proposed method, two approaches have been presented through analytical and simulation based approaches. Different islanding and non-islanding cases such as short circuit faults, capacitor bank switching and load changes in various values and locations of the test systems have been studied. In addition, the proposed method has been compared with both ROCOF and ROCOFOP methods and it has been shown that the proposed method for active power mismatches smaller than 10% has better performance and for larger than 10%, because of existing OFP/UFP in structure of proposed method as back up protection, the same capability of both ROCOF and ROCOFOP methods has been established.

Appendix

A. Simplified Swing Equation

The following equation presents the swing equation [30, 31]:

$$\frac{2H}{\omega_b}\frac{d^2\delta}{dt^2}+D\frac{d\delta}{dt}=P_m-P_{\max}\sin(\delta) \qquad (A-1)$$

If a part of the system encountered with a disturbance and the rotor angle (δ) has a small variation, the following equation can be written:

$$\frac{2H}{\omega_b}\frac{d^2}{dt^2}(\delta_0+\Delta\delta)+D\frac{d}{dt}(\delta_0+\Delta\delta) = P_m-P_{\max}\sin(\delta_0+\Delta\delta) \qquad (A-2)$$

This equation can be rewritten, as follows:

$$\frac{2H}{\omega_b}\frac{d^2\delta_0}{dt^2}+\frac{2H}{\omega_b}\frac{d^2\Delta\delta}{dt^2}+D\frac{d\delta_0}{dt}+D\frac{d\Delta\delta}{dt} = P_m-P_{\max}\left[\sin\delta_0\cos\Delta\delta+\sin\Delta\delta\cos\delta_0\right] \qquad (A-3)$$

If the rotor angle deviation has a small variation ($\Delta\delta \le 10^{\circ}$), by substituting sin ($\Delta\delta$) with $\Delta\delta$ and cos ($\Delta\delta$) with 1, the above mentioned equation is converted to the following two simple equations. The first equation (i.e., (A–4)) expresses the behavior of the power system in steady state condition and the second one (i.e., (A–5)) expresses the transition state of the synchronous generator.

$$\frac{2H}{\omega_b}\frac{d^2\delta_0}{dt^2}+D\frac{d\delta_0}{dt}=P_m-P_{\max}\sin(\delta_0) \qquad (A-4)$$

$$\frac{2H}{\omega_b}\frac{d^2\Delta\delta}{dt^2}+D\frac{d\Delta\delta}{dt}=-P_{\max}\cos(\Delta\delta) \qquad (A-5)$$

References

[1] Beiza J., Hosseinian S. H. and Vahidi B., "Fault Type Estimation in Power Systems", *Iranian Journal of Electrical & Electronic Engineering,* Vol. 5, No. 3, pp. 185-195, September 2009.

[2] Golkar M. A. and Gahrooyi Y. R., "Stochastic Assessment of Voltage Sags in Distribution Networks", *Iranian Journal of Electrical & Electronic Engineering*, Vol. 4, No. 4, pp. 191-201, January 2008.

[3] IEEE Standard for Interconnecting Distributed Resources with Electric Power Systems, *IEEE Std.* 1547–2003, July 2003.

[4] Massoud M., Ahmed K. H., Finney S. J. and Williams B. W., "Harmonic distortion–based Island detection technique for inverter–based distributed generation", *Inst. Eng. Technol. Renew. Power Gen*., Vol. 3, No. 4, pp. 493-507, 2009.

[5] Jang S. and Kim K. H., "An Islanding Detection Method for Distributed Generations Using Voltage Unbalance and Total Harmonic Distortion of Current", *IEEE Transaction on power delivery*, Vol. 19, No. 2, pp. 745-752, 2004.

[6] Wang W., Kliber J., ZHang G., XU W., Howell B. and Palladino T, "A power line signaling based scheme for anti-islanding protection of distributed generators - Part II: field test results", *IEEE Transaction on power delivery*, Vol. 22, No. 2, pp. 1767-1772, 2007.

[7] Davidson E. M., Mcartur S. D. J., Mcdonald J. R., Cumming T. and Watt I., "Applying multi-agent system technology in practice: automated management and analysis of SCADA and digital fault recorder data", *IEEE Transaction on power systems*, Vol. 21, No. 2, pp. 559-567, 2006.

[8] Vahedi H., Noroozian R., Jalilvand A. and Gharehpetian G. B., "A New Method for Islanding Detection of Inverter-Based Distributed Generation Using DC-Link Voltage Control", *IEEE Transaction on power delivery,* Vol. 26, No. 2, pp. 1176-1186, 2011.

[9] Du P., Nelson J. K. and Ye Z., "Active anti-islanding schemes for synchronous machine-based distributed generators", *IEE Proc. Gener.*

Transm. Distrib., Vol. 152, No. 5, pp. 597-606, 2005.

[10] Bahrani B., Karimi H. and Iravani R., "Nondetection Zone Assessment of an Active Islanding Detection Method and its Experimental Evaluation", *IEEE Transaction on power delivery*, Vol. 26, No. 2, pp. 517-525, 2011.

[11] Lopes L. and Sun H., "Performance assessment of active frequency drifting islanding detection methods", *IEEE Transaction on Energy Conversion.*, Vol. 21, No. 1, pp. 171-180, 2006.

[12] Vieira J. C. M., Freita W., Xu W. and Morelato A., "Efficient Coordination of ROCOF and Frequency Relays for Distributed Generation Protection by Using the Application Region", *IEEE Transaction on power delivery*, Vol. 21, No. 4, pp. 1878-1884, 2006.

[13] Sadeh J. and Kamyab E., "Inverter based distributed generator islanding detection method using U/O voltage relay", *Iranian Journal of Electrical & Electronic Engineering*, Vol. 8, No. 4, pp. 311-321, 2012.

[14] Vieira J. C. M., Salles V. D. and Freitas W., "Power imbalance application region method for distributed synchronous generator anti-islanding protection design and evaluation", *International Journal of Electric Power System Research*., Vol. 81, No. 10, pp. 1952-1960, 2011.

[15] Freitas W., Huang Zh. and Xu W., "A Practical Method for Assessing the Effectiveness of Vector Surge Relays for Distributed Generation Applications", *IEEE Transaction on power delivery*, Vol. 20, No. 1, pp. 57-63, 2005.

[16] Pai F. S. and Huang Sh. J., "A Detection Algorithm for Islanding-Prevention of Dispersed Consumer-Owned Storage and Generating Units", *IEEE Transaction on Energy Conversion.*, Vol. 16, No. 4, pp. 346-351, 2001.

[17] Samui A. and Samantaray S. R., "Assessment of ROCPAD Relay for Islanding Detection in Distributed Generation", *IEEE Transaction on Smart Grid.*, Vol. 2, No. 2, pp. 391-398, 2011.

[18] Zeineldin H. H. and Kirtley J. L., "A Simple Technique for Islanding Detection with Negligible Nondetection Zone", *IEEE Transaction on power delivery*, Vol. 24, No. 2, pp. 779-786, 2009.

[19] Moeini A., Darabi A., Rafiei S. M. R. and Karimi M., "Intelligent islanding detection of a synchronous distributed generation using governor signal clustering", *International Journal of Electric Power System Research*, Vol. 81, No. 2, pp. 608-616, 2010.

[20] Liserre M., Pigazo A., Dell'Aquila A. and Moreno V.M., "An Anti-Islanding Method for Single-Phase Inverters Based on a Grid Voltage Sensorless Control", *IEEE Transaction on Industrial Electronics.*, Vol. 53, No. 5, pp. 1418-1426, 2006.

[21] Najy W. K. A., Zeineldin H. H., Alaboudy A. H. K. and Woon W. L., "A Bayesian Passive Islanding Detection Method for Inverter-Based Distributed Generation Using ESPRIT", *IEEE Transaction on power delivery*, Vol. 26, No. 4, pp. 2687-2696, 2011.

[22] Zeineldin H. H., Abdel-Galil T., Elsaadany E. F. and Salam M. M. A., "Islanding detection of grid connected distributed generators using TLS-ESPRIT", *International Journal of Electric Power System Research*, Vol. 77, No. 2, pp. 155–162, 2006.

[23] Vahedi H. and Karrari M., "Adaptive Fuzzy Sandia Frequency-Shift Method for Islanding Protection of Inverter-Based Distributed Generation", *IEEE Transaction on power delivery*, Vol. 28, No. 1, pp. 84-92, 2013.

[24] Vahedi H., Gharehpetian G. B. and Karrari M., "Application of Duffing Oscillators for Passive Islanding Detection of Inverter-Based Distributed Generation Units", *IEEE Transaction on power delivery*, Vol. 27, No. 4, pp. 1973-1983, 2012.

[25] Arroudi K. E., Joós G., Kamwa I. and Mc Gillis D. T., "Intelligent-Based Approach to Islanding Detection in Distributed Generation", *IEEE Transaction on power delivery*, Vol. 22, No. 2, pp. 828-835, 2007.

[26] Lidula N. W. A. and Rajapakse A. D., "A Pattern Recognition Approach for Detecting Power Islands Using Transient Signals-Part I: Design and Implementation", *IEEE Transaction on power delivery*, Vol. 25, No. 4, pp. 3070-3077, 2010.

[27] Mahat P., Chen Z. and Jensen B. B., "A Hybrid Islanding Detection Technique Using Average Rate of Voltage Change and Real Power Shift", *IEEE Transaction on power delivery*, Vol. 24, No. 2, pp. 764-771, 2009.

[28] Khattam W. E., Sidhu T. S. and Seethapathy R., "Evaluation of Two Anti-Islanding Schemes for a Radial Distribution System Equipped With Self–Excited Induction Generator Wind Turbines", *IEEE Transaction on Energy Conversion.*, Vol. 25, No. 1, pp.107-117, 2010.

[29] Best R. J., Morrow D. J., Laverty D. M. and Crossley P. A., "Techniques for Multiple-Set Synchronous Islanding Control", *IEEE Transaction on Smart Grid.*, Vol. 2, No. 1, pp. 60-67, 2011.

[30] Anderson P. M. and Fouad A. A., "power system control and stability", Ames, IA: the Iowa state university press, 1977, pp. 13-148.

[31] Kundur P., "Power System Stability and Control", New York, McGraw-Hill Inc, 1994.

[32] Ogata K., "Modern Control Engineering", New Jersey, Prentice Hall, 1997.

Mohsen Bakhshi was born in Iran in1987. He received the B.Sc. and the M.Sc. degrees in electrical engineering from Zanjan University, Zanjan, Iran, in 2010 and 2012, respectively. His research interests include distributed generation, power electronics, power system operation, and artificial intelligence.

Reza Noroozian was born in Iran. He received the B.Sc. degree from Tabriz University, Tabriz, Iran, in 2000, and the M.Sc. and Ph.D degrees in electrical engineering from Amirkabir University of Technology, Tehran, Iran, in 2003 and 2008, respectively. He is an Assistant Professor with the Department of Power Engineering at The University of Zanjan, Zanjan, Iran. His areas of interest include power electronics, power systems, power quality, integration and control of renewable generation units, custom power, micro grid operation, distributed-generation modeling, as well as operation and interface control.

G. B. Gharehpetian received his BS, MS and Ph.D. degrees in electrical engineering in 1987, 1989 and 1996 from Tabriz University, Tabriz, Iran and Amirkabir University of Technology (AUT), Tehran, Iran and Tehran University, Tehran, Iran, respectively, graduat-ing all with First Class Honors. As a Ph.D. student, he has received scholarship from DAAD (German Academic Exchange Service) from 1993 to 1996 and he was with High Voltage Institute of RWTH Aachen, Aachen, Germany. He has been holding the Assistant Professor position at AUT from 1997 to 2003, the position of Associate Professor from 2004 to 2007 and has been Professor since 2007. He was selected by the ministry of higher education as the distinguished professor of Iran and by IAEEE (Iranian Association of Electrical and Electronics Engineers) as the distinguished researcher of Iran and was awarded the National Prize in 2008 and 2010, respectively. Prof. Gharehpetian is the author of more than 630 journal and conference papers. His teaching and research interest include power system and transformers transients and power electronics applications in power systems.